CHAPTER 7
ABSOLUTE MOTION OF EARLY CRETACEOUS PACIFIC PLATE

7-1. Plate Tectonics

Gordon (1995) describes that plate motions are Earth's most important tectonic processes, because a tectonic plate moves on the nearly spherical surface of Earth and because a plate works as excellent approximation to be rigid, and plate motions can be represented simply as rigid body rotations. In the limiting case of geologically recent motion, the time derivative of rigid-body rotation can be described by angular velocity, which is an axial vector. The assumption of plate rigidity allows geometrically precise and rigorously testable predictions to be made. The observed near rigidity of the plates also permits the treatment of plate kinematics separately from dynamics. Abundant data describe the geologically recent motion across narrow boundaries linking nearly all the major plates, permitting many tests of plate tectonic predictions (Gordon, 1995) (Figure 7.1).

The plate tectonic data of geologically recent plate motions depend mainly on three types data as follows;

- Spreading rates estimated from the observed spacing of magnetic anomaly data.
- The azimuth of a submarine transform fault estimated from bathymetric observations.
- The azimuth of slip calculated from a focal mechanism inferred from the radiation pattern of seismic waves from an Earthquake along a transform fault or at a trench.

Global plate motion models completely specify the motion between the plates. As such, there is no need to specify the motion of the plates relative to an external frame, which is stationary relative to any one plate.

Different geological and dynamical assumptions have been proposed for specifying the motion of the plates relative to the mesosphere. Motion relative to the mesosphere is often referred to as "absolute plate motion". Absolute plate motion can be estimated by assuming that various hotspots are stationary relative to one another and to the mesosphere, possibly because they are rooted in deep mantle plumes that originate in the comparatively non-deforming deep mantle (Morgan, 1972; Wilson, 1963). Age progressions and trends of linear seamount chain or island chain reflect motion between the plates and mesosphere (see chapter 1.4).

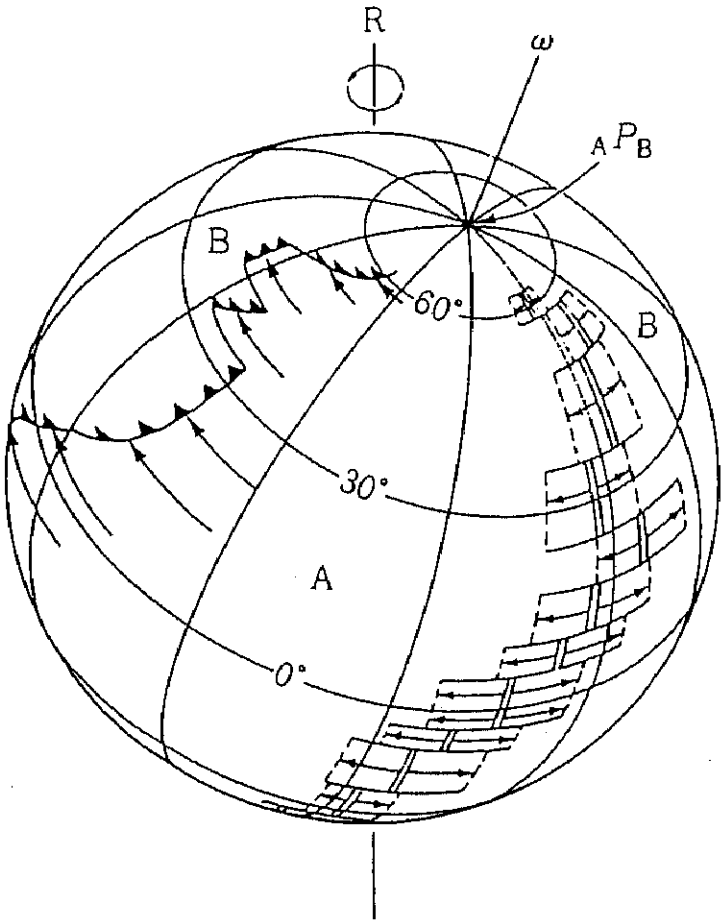

Figure 7.1 The Euler pole calculated from plate motions. Some accounts are R: north pole of the Earth, $_AP_B$: Euler rotation pole of a relative plate motion between plate A and B bounded by divergent and convergent margins, ω: an angular velocity of the Euler rotation pole $_AP_B$. Arrows show vectors of relative plate motion. Adopted from Sugimura *et al.* (1988).

7-2 Calculating Rotation Pole

Absolute plate motion can be estimated by assuming that various volcanic hotspots are stationary relative to one another and to the mesosphere, possibly because they are rooted in deep mantle plumes that originate in the comparatively non-deforming deep mantle (Morgan, 1972; Wilson, 1963). On these assumptions age progressions and trends of collinear chains reflect motion between the plates and mesosphere.

This theorem states that any line of the surface of a sphere can be translated to any other position and orientation on the sphere by a single rotation about a suitably chosen axis passing through the center of the sphere. In terms of the Earth this means that a rigid surface plate can be shifted to a new position by a rotation about a uniquely defined axis. The point where this axis intercepts the surface of the Earth is known as a pole rotation (Gordon, 1995). This is illustrated in Figure 7.2, where an oceanic plate is rotating with respect to hotspots.

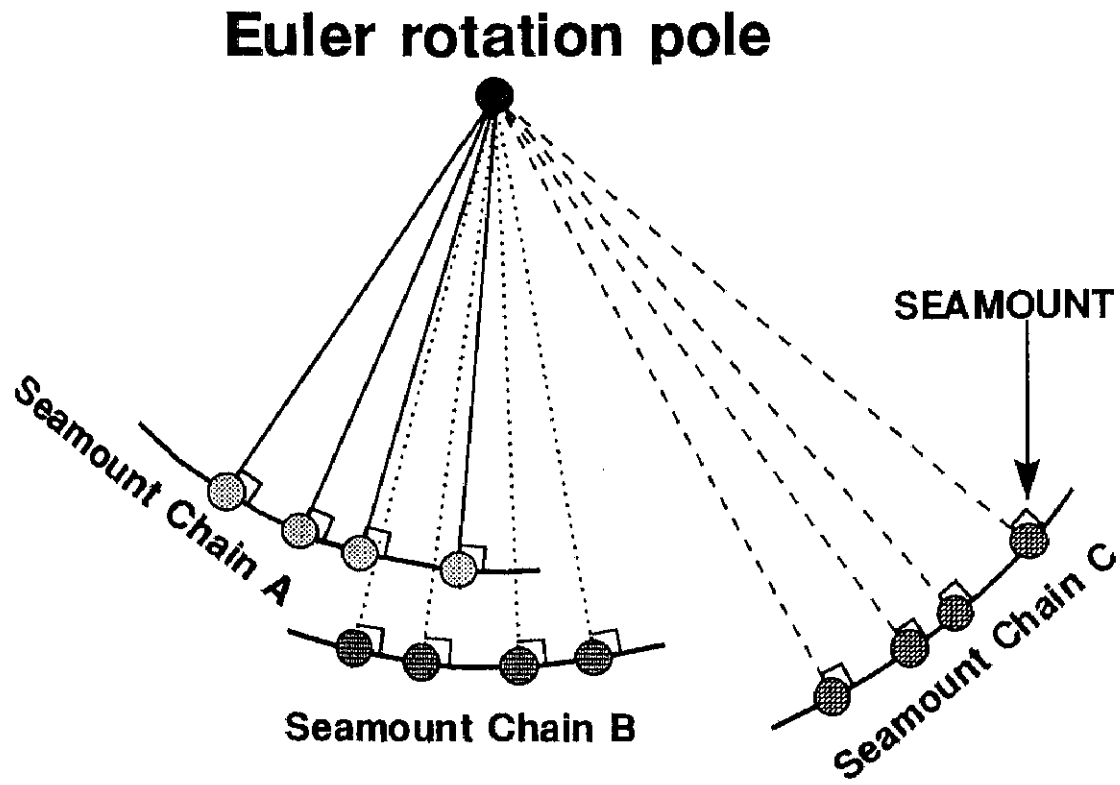

Figure 7.2 Euler rotation pole based on the location and trace of seamount chains.

For the calculation of Euler rotation poles, the three points, χ_A and χ_B of the latitude θ_A, θ_B, east longitude ϕ_A, ϕ_B, and geographic north pole are used (Figure 7.3). Adopted from Turcotte (1982), using the laws of sines and cosines in the spherical trigonometry of Figure 7.3, we can write the formulae as follows:

$$\sin\Delta = \cos(90°-\theta_A)\cdot\cos(90°-\theta_B) + \sin a\cdot\sin b\cdot\cos|\psi_A - \psi_B| \qquad [7\text{-}1]$$

$$\frac{\sin(90°-\theta_A)}{\sin B} = \frac{\sin(90°-\theta_B)}{\sin A} = \frac{\sin\Delta}{\sin|\psi_A - \psi_B|} \qquad [7\text{-}2]$$

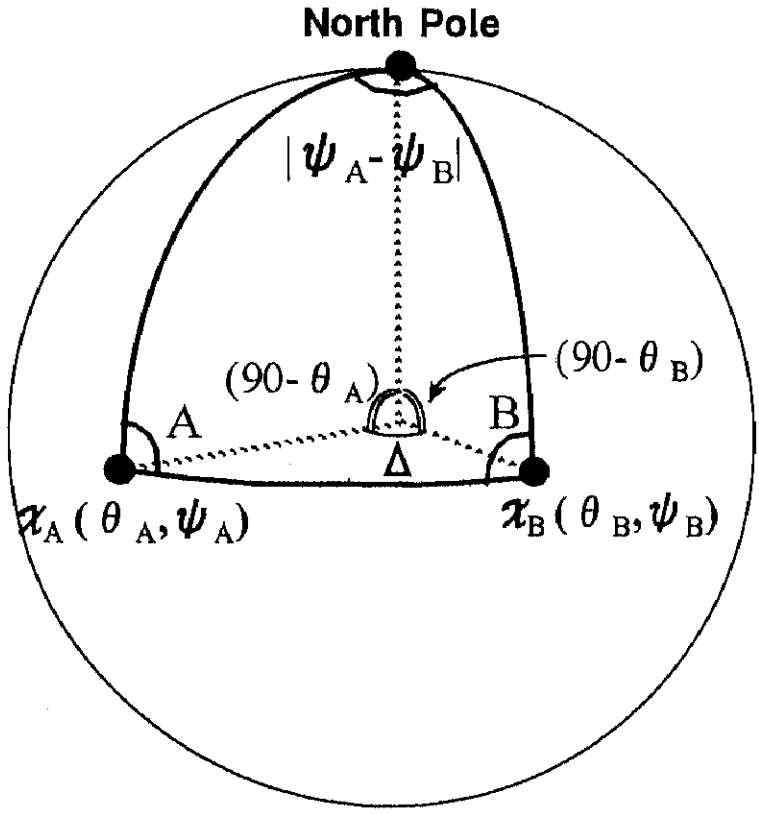

Figure 7.3 A spherical trigonometry by the points of χ_A, χ_B and the geographic north pole.

We can obtain the Δ, A and B. The surface distance s between A and B is

$$s = r \cdot \Delta \qquad [7\text{-}3]$$

where r is the radius of the Earth with Δ in radians. This relation along with equations [7-1] and [7-3] can be used to determine the distance between two points on the surface of the Earth.

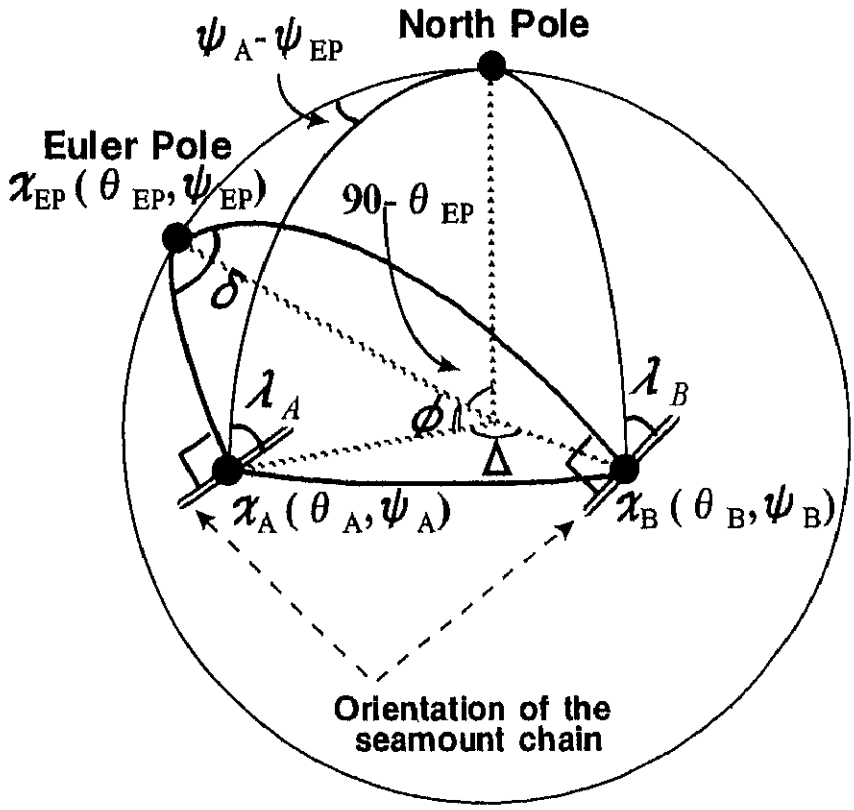

Figure 7.4 The spherical trigonometry by the points of χ_A, χ_B and the Euler rotation pole. Each seamount chain of the points of χ_A, χ_B must be vertical against the directions to the rotation pole.

When the orientations of seamount chain against the north in two points of x_A and x_B are λ_A and λ_B, respectively in Figure 7.4, we have the following formulae:

$$\angle x_{EP}x_Ax_B = 90°-\lambda_A + A \qquad [7\text{-}4]$$

$$\angle x_{EP}x_Bx_A = B-(90°-\lambda_B) \qquad [7\text{-}5]$$

Reusing the laws of sines and cosines in another spherical trigonometry, x_A, x_B and rotation pole of Figure 7.4, we can write the formulae as follows:

$$\begin{aligned}\cos\delta = &-\cos\{B-(90°-\lambda_B)\}\cdot\cos(90°-\lambda_A + A)\\ &+\sin\{B-(90°-\lambda_B)\}\cdot\sin(90°-\lambda_A + A)\cdot\cos\Delta\end{aligned} \qquad [7\text{-}6]$$

$$\frac{\sin\phi}{\sin\{B-(90°-\lambda_B)\}} = \frac{\sin\Delta}{\sin\delta} \qquad [7\text{-}7]$$

We can obtaine the δ from the formula [7-6] and ϕ from the formula [7-7]. By the laws of sines in another spherical trigonometry, x_A, geographic north pole and rotation pole of Figure 7.4, we can write the formulae as follows:

$$\begin{aligned}\cos(90°-\theta_{EP}) = &\cos\phi\cdot\cos(90°-\psi_A)\\ &+\sin\phi\cdot\sin(90°-\psi_A)\cdot\cos(90°-\lambda_A)\end{aligned} \qquad [7\text{-}8]$$

$$\frac{\sin(\psi_A - \psi_{EP})}{\sin\phi} = \frac{\sin(90°-\theta_{EP})}{\sin(90°-\lambda_A)} \qquad [7\text{-}9]$$

The latitude and longitude of Euler pole, θ_{EP} from the formula of [7-8] and Ψ_{EP} from the formulae of [7-8] and [7-9] are obtained.

The angular velocity of rotation, ω, is reached the following fomula:

$$v = \omega \cdot r \cdot \sin\phi \qquad [7\text{-}10]$$

where r is the radius of the Earth, and ϕ is the angle subtended at the center of the Earth by the pole of rotation and the point χ (Figure 7.4). As v is as the absolute velocity on the point χ, the plural angular velocities, ω, are calculated in each point.

7-3 Early Cretaceous Euler Pole

In this paper, we can use the two trails; one is from the Fukunaga and Hemler Seamounts in the Magellan Seamount Chain, and another is from the Shatsky Rise as the Early Cretaceous seamount chains on the Pacific Plate. In this thesis the Mid-Pacific Mountains should not adopt as a Early Cretaceous hotspot track, at which the data is used by Duncan and Clague (1985) and Engebretson et al. (1985), because the formation ages of the Mid-Pacific Mountains are based on the fossil ages of sedimentary rocks (Heezen, 1973). On the other hand, at the Late Jurassic to Early Cretaceous Shatsky Rise, no radiometric ages have been obtained, but the paleomagnetic age are clearly established (Nakanishi *et al.*, 1989) (see chapter 1-4).

The data of two points for calculating the Early Cretaceous Euler rotation pole are shown in Table 7.1 and Figure 7.5.

Table 7.1 Calculated values at two trails as a Early Cretaceous Euler rotation pole.

Seamount Chain	Point	Age	Latitude	Longitude	Orientation of seamount trail
		Ma	θ	Ψ	λ
Magellan Trail	Fukunaga Seamount	before 140	15°29	147°50	42°13 NE
	Hemler Seamount	130 to 120	19°33	151°34	
Shatsky Trail	Chron M16 bending	140.5	37°15	161°00	44°05 NE
	Chron M9 bending	130	40°20	164°15	

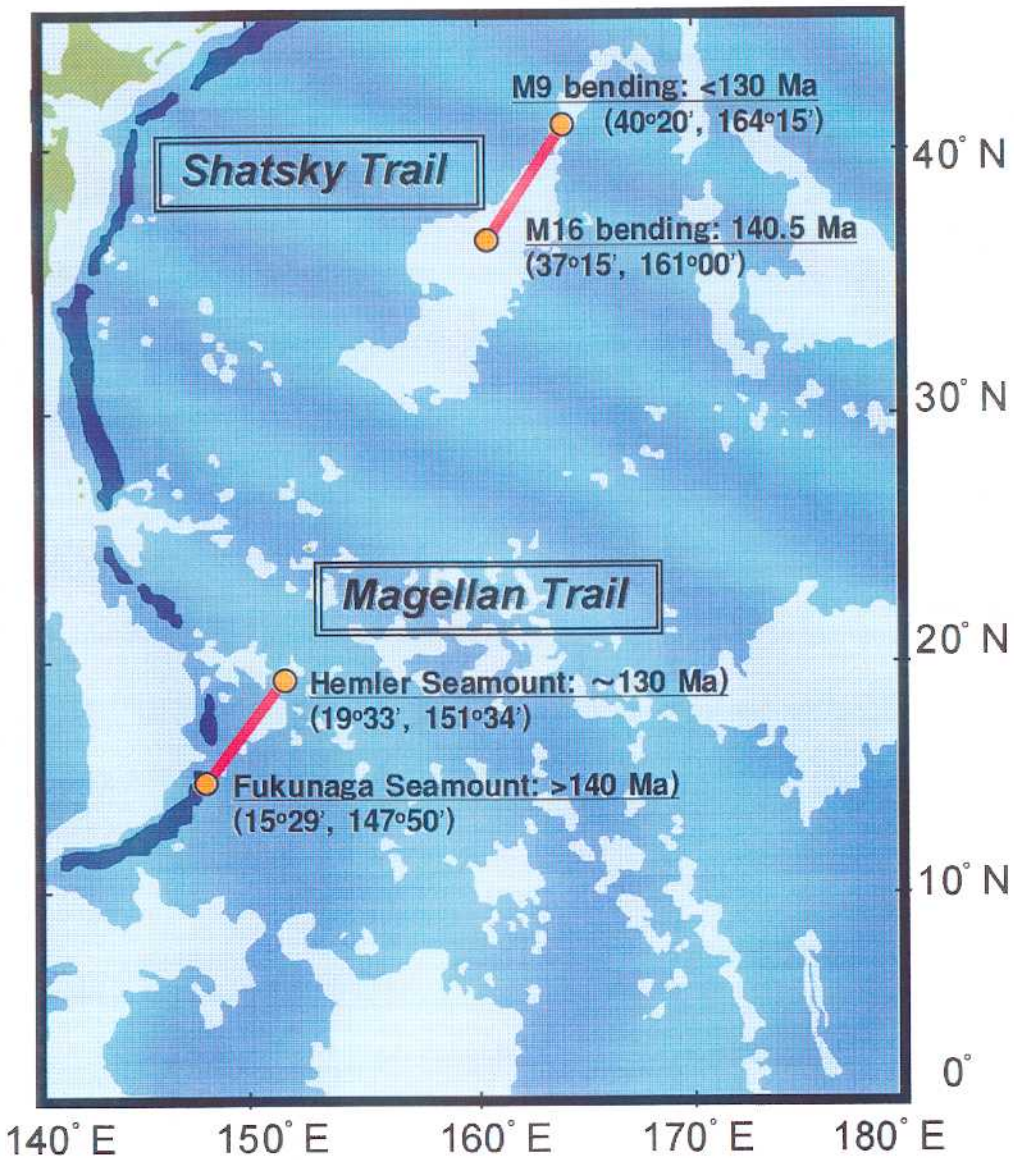

Figure 7.5 Data and site calculated for determination of the Early Cretaceous Euler rotation pole. Shatsly Rise and Hemler Seamount are referred to Naknishi *et al.* (1999) and Smith *et al.* (1989), respectively. The Fukunaga Seamount in the Magellan Seamount Chain is in this study.

The calculation result of the Early Cretaceous Euler pole is shown in Table 7.2. As mentioned chapter 1-3, the pole reported by Duncan and Clague (1985) is only one before 100 Ma using only a few fossil ages of the Mid-Pacific Mountains. This thesis should not adopt this. The calculated two angular velocity in this study were indicated from the Magellan Seamount Chain and the Shatsly Rise. The angular velocity shown in Table 7.2 is an average value.

This pole is on a great circle of perpendicular line against the Shatsly Trail and the Magellan Trail on the suface of the Earth. The Euler poles during this time reported by the Koppers (1998MS) and Engebretson *et al.* (1985) are also on the same great circle (Figure 7.6). But they are calculated from only one seamount trails, respectively. Newly calculated Early Cretaceous Euler pole must be more precise.

Table 7.2 Calculated and reported Euler poles.

Stage Pole (Ma)	Latitude (^{o}N)	Longitude (^{o}E)	Angular Velocity (degree/Myr)	Source
125-140	7.7	33.1	0.20	Koppers (1998MS)
123-132	36.7	344.1	0.54	Engebretson et al. (1985)
132-154	32.5	61.2	0.32	Engebretson et al. (1985)
100-150	85.0	15.0	0.48	Duncan and Clague (1985)
120-140	40.3	103.7	0.33	This Study

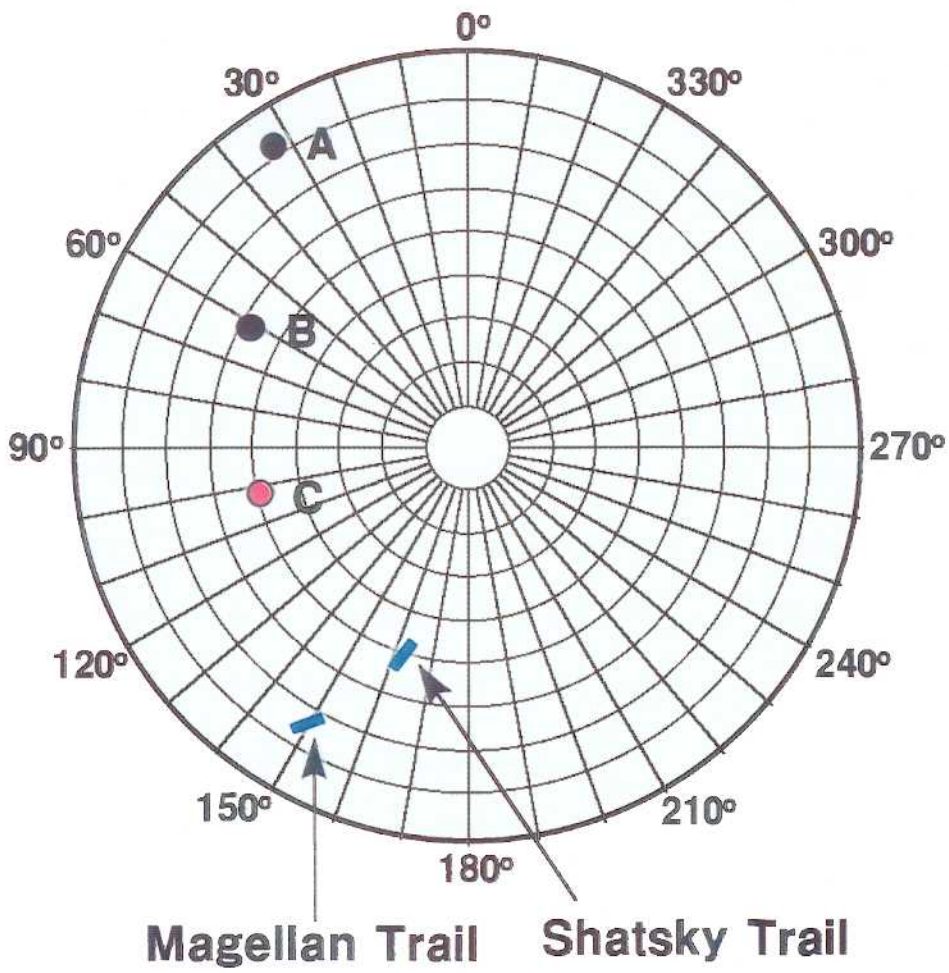

Figure 7.6 Calculated Early Cretaceous Euler rotation pole obtained in this study (C). Other Euler poles A and B are calculated by Koppers (1998MS) and Engebretson *et al.* (1985), respectively. All rotation poles are on the vertical circle against seamount trails.